International Journal of Fluid Power 14 (2013) No. 1 pp. 17-23

EXPERIMENTAL OBSERVATIONS OF THE FLUID FLOW WITHIN THE L-SHAPED CHECK VALVE

Shinji Kajiwara

Kinki University, Department of Mechanical Engineering, 3-4-1 Kowakae, Higashiosaka, Osaka, Japan
kajiwara@mech.kindai.ac.jp

Abstract

The spring-driven ball-type check valve is one of the most important components of hydraulic systems: it controls the position of the ball and prevents backward flow. To simplify the structure, the spring must be eliminated, and to accomplish this, the flow pattern and the behavior of the check ball in L-shaped pipe must be determined. In this paper, we present a full-scale model of a check ball made of acrylic resin, and we determine the relationship between the initial position of the ball, the diameter of the inflow port, and the kinematic viscosity of oil. When kinematic viscosity is high, the check-flow rate increases in a standard center inflow model, and it is possible to greatly decrease the check-flow rate by shifting the inflow from the center.

Keywords: hydraulics, pipe flow, experimental analysis, flow visualization, check ball, L-shaped pipe

1 Introduction

Hydraulic systems are used for work that requires linear and rotational motion, large forces, and freely changeable speed, and the advancement of hydraulic technology has allowed it to be used as a means of energy transfer not only in construction and civil engineering equipment but also in products more closely associated with our daily lives such as automobiles, airplanes, and elevators. One of the important components of a hydraulic system is the check valve. Most check valves that use a ball also generally use a spring to push on the ball to regulate its position to reliably prevent back flow. There is a strong desire, however, to eliminate the spring because of the problem of it being broken by the chattering of the ball and to reduce costs. In addition, the shapes of the piping used around the check valve are the straight type and the L-shaped elbow type. Testing and analytical research are being conducted on the shape of the straight type check valves (Hong, 2002; Tsukiji, 1996). Further, research, eigenvalue analysis, and three-dimensional numerical analysis, etc., are being conducted on poppet valves (Hayase, 1992). The simulation method of fluid power systems is developed and discusses several analysis results in detail by comparing simulation results with actual measurement results (Grossschmidt, 2009).

This manuscript was received on 09 May 2012 and was accepted after revision for publication on 30 October 2012

The check ball behavior of hydraulic check valves with L-shaped piping in terms of the hydraulic fluid flow and the effect on check ball behavior of that flow, etc., have not been clarified to date. The flow in the pipe applies hydrodynamic force to the ball causing the flow around the check ball to become a more complex flow and bend further to the perpendicular.

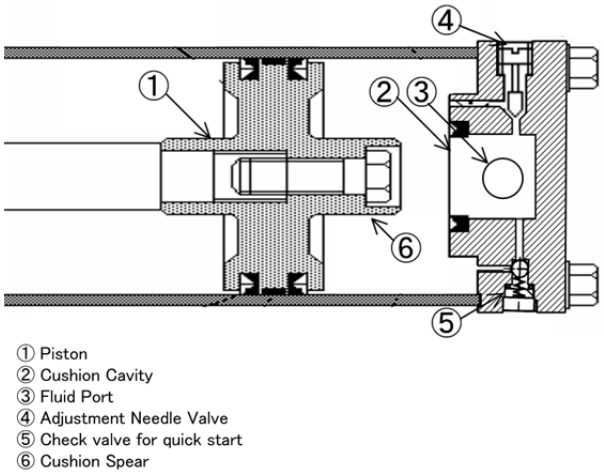

Fig. 1: *Schematic view of dumper cylinder*

The behavior of the check ball at this time is subject to the complex relationship between flow path relative position relationship and the flow rate, viscosity, and

other factors. For this research we used transparent acrylic models of actual check valves to observe the check valve behavior while respectively changing the ball position, flow rate, and viscosity and to study the check ball behavior and the check flow rate at which the check valve can reliably prevent back flow. For the models we used two types with different inlet diameters and positions as the test pieces. Please note the when the check ball in the hydraulic pipe was used as a check valve, the pressure difference was made small and the model was made of acrylic to provide good visibility.

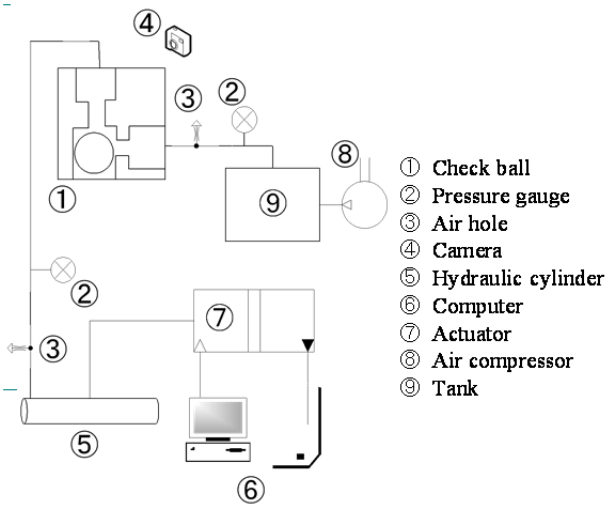

Fig. 2: *Experimental apparatus*

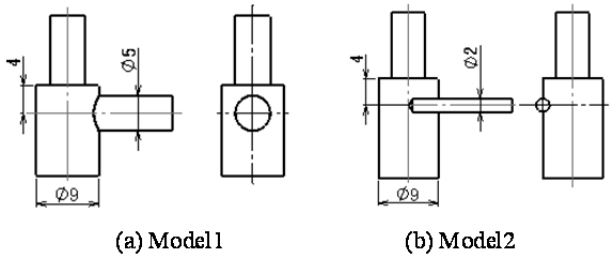

Fig. 3: *L-shaped pipe arrangement*

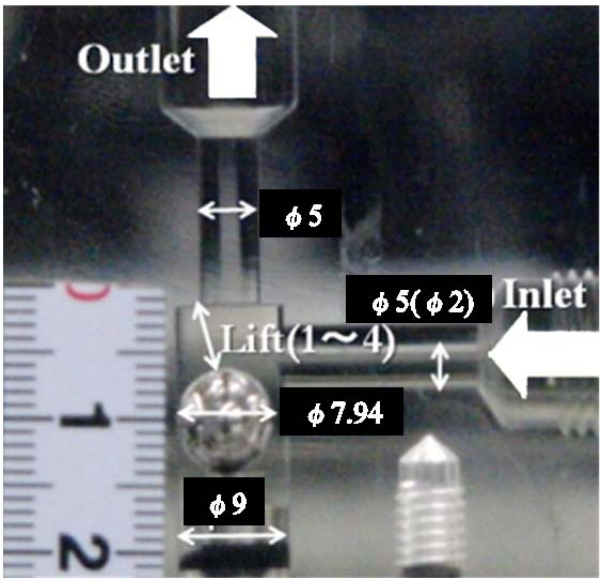

Fig. 4: *Experimental model*

2 Test Apparatus and Method

The example of the usage of the check ball of hydraulic check valves with L-shaped piping is shown in Fig. 1. Cushions are small diameter pistons (6) that enter a small cavity (2) machined into the end caps. Cylinder heads with cushions usually have a built in check valve (5) that allows the free flow of hydraulic fluid into the cylinder so that the speed of the cylinder will not be limited when the direction of travel is reversed. Cylinders with adjustable cushions will have needle valves (4) mounted in the heads so that the flow of fluid leaving the cushion can be adjusted and the amount of deceleration can be tuned for the application.

A schematic diagram of the test apparatus is shown in Fig. 2. The computer (6) controls the head speed of the servo actuator (7). The hydraulic cylinder (5) is connected to the actuator and operated to determine the flow rate of the acrylic plastic L-shaped pipe sample (1). Pressure of 100 kPa is applied to the hydraulic fluid tank of (9) to prevent air from being sucked into the hydraulic fluid. The test confirmed the check ball rises and can be checked, and the 300 fps high-speed camera of (4) was used to observe the ball to measure its rotation. Because images were used to measure the rotation, the ball was marked with six plus (+) laser markers. The test parameters were the initial position of the check ball, the hydraulic fluid kinetic viscosity, and the hydraulic fluid check flow rate. For the model shapes, Model 1, the reference model, uses a φ9 cylinder containing a 7.94 mm check ball and allowing inflow and outflow via a φ5 orifice, and Model 2 was modified by reducing the inflow orifice to φ2 and shifting the inflow position to the side so that the swirling flow of the hydraulic fluid would cause the ball to rotate. Models 1 and 2 are shown in Fig. 3(a) and 3(b), respectively. To regulate the check ball initial position, the average distance from the outflow edge of the L-shaped pipe to the ball is defined as the shift amount. The shift amount was determined by regulating the ball bottom position while filming the ball from 2 directions using digital cameras. The construction around the L-shaped pipe is shown in Fig. 4. The check ball initial position was tested using shift amounts of 1, 2, 3, and 4 mm. In addition, 3 hydraulic fluid kinetic viscosities of 6 mm^2/s, 15 mm^2/s, and 35 mm^2/s, which are within the general hydraulic fluid range, were used, and the check flow rate was tested in the range of 0 to 60 cm^3/s (0 to 6.0 $\times$ $10^{-5} m^3/s$). For the test each of these was conducted 5 times and evaluated by taking the average for the check flow rate and the rotational speed.

The Reynolds number Re is expressed using the flow velocity in the inlet pipe. The inlet diameter (2 mm or 5 mm) is used for the reference length when calculating the Reynolds number.

3 Test Results

The ball rise as well as the relationship between the checkable check flow rate and lift obtained from the test are shown in Fig. 5. Since the check flow rate was

very reproducible and the error was within 5 % percent, the average value for it is shown. As can be seen in this figure, for the Model 1 center inflow, little change is caused in the check flow rate by the change in the kinetic viscosity at a lift of 1 mm and is less than 8.3 cm^3/s. As the lift increases, the check flow rate also increases, and it can be seen that at a lift of 3 mm a check flow rate of about 20 cm^3/s is required. During the lift from 1 mm to 3 mm the check flow rate decreased accompanying the increase in kinetic viscosity. For a lift of 4 mm, however, the change in kinetic viscosity had a large effect on the check flow rate. In other words, we observed that when the kinetic viscosity was 15 mm^2/s the maximum check flow rate was 52 cm^3/s. In the case of Model 2, making the flow inlet smaller and offsetting its position greatly reduced the check flow rate and within the range performed during the test the check flow rate was lowered below 8.3 cm^3/s. The main reason for this is thought to be the decrease in the hydraulic fluid reactive force, in other words the force pressing downward on the ball, that is generated when the flow is changed to upward by shifting the flow inlet. In Model 2, both the kinetic viscosity and the lift had only a very small effect on the check valve flow.

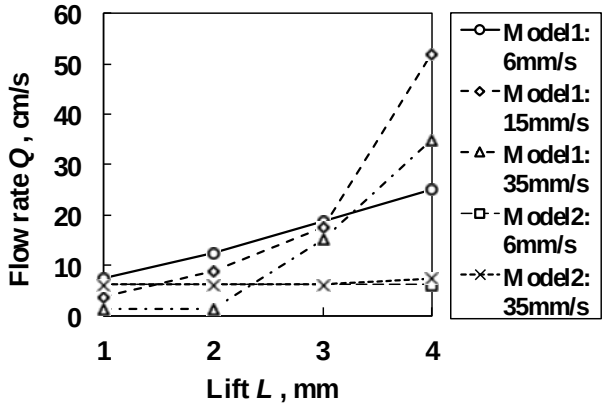

Fig. 5: *Relationship between lift L and check flow rate*

Next, the relationship between the kinetic viscosity and the check flow rate for Models 1 and 2 is shown in Fig. 6(a) and 6(b).

Figure 6 shows that when the lift is 3 mm or less, as the kinetic viscosity increases, the check flow rate must be larger. However, it also shows that when the lift is 4 mm, the greatest check flow rate is required when the kinetic viscosity is 15 mm^2/s. The reason for this is thought to be that when the ball position is lower than the inflow location, the fluid jet strikes the top of the ball and thus applies a downward force to it, which increases the check flow rate.

As the kinetic viscosity increases, however, the viscous force of the rising main stream increases and thus the balance between the downward force and the viscous force is thought to decrease the check flow rate. The Reynolds number Re is below 1,000 in all cases and thus is close to a laminar flow state, so it is assumed the effect of the kinetic viscosity from the laminar flow boundary layer is large. In model 2, however, the effect of the kinetic viscosity was very small. The Reynolds number also had a range from about 150 to 1,700, and the flow is assumed to be in a laminar flow state in all cases. Model 2 generates a swirling flow in the check ball range, but the effect on the ball buoyancy from the change in kinetic viscosity is small. The test on Model 2 showed that the strength of the swirling flow around the ball had a large effect on the ball's buoyancy. Here, the flow rate and kinetic viscosity were changed and the rotational speed of the ball was measured using a high-speed camera. The results of measuring the rotational speed at a lift of 1 mm are shown in Fig. 7(a) and that for lifts of 2, 3, and 4 mm is shown in Fig. 7(b), 7(c), and 7(d), respectively. From Fig. 6 it can be seen that as the kinetic viscosity increases, the rotational speed decreases. In other words, the smaller the kinetic viscosity, the higher the rotational speed of the ball, which increases the check flow rate. This also shows that the flow rate and rotational speed have a nearly proportional relationship. The relationship between the rotational speed and the lift at a kinetic viscosity of 6 mm^2/s is shown in Fig. 8(a), and the relationship between the rotational speed and the lift at a kinetic viscosity of 15 mm^2/s is shown in Fig. 8(b). The rotational speed becomes lower at the comparatively high viscosity of 15 mm^2/s, but the check flow rate also became smaller. This is thought to be due to an increasing upward force on the surface of the ball accompanying the decrease in swirling flow generated around the ball as the hydraulic fluid viscosity increases.

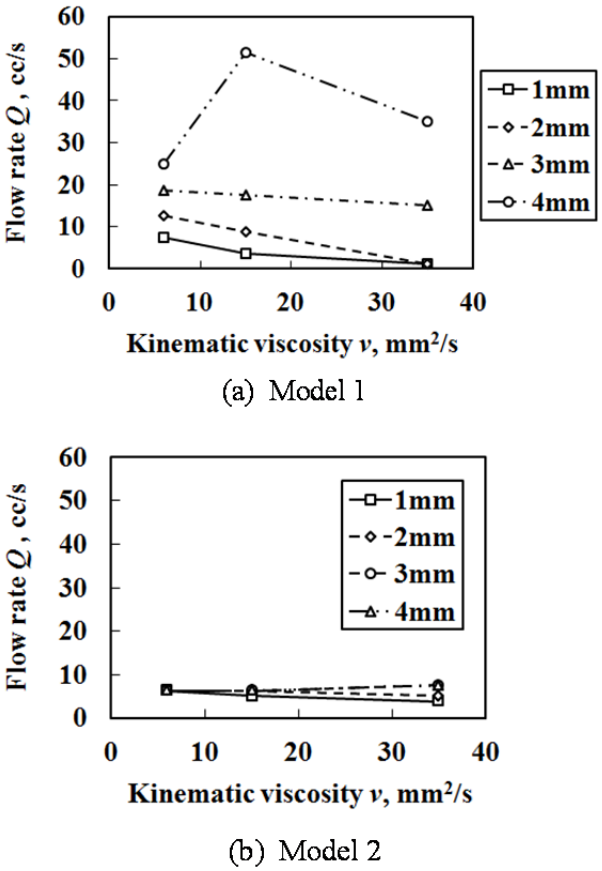

Fig. 6: *Relation between kinetic viscosity v and flow rate Q*

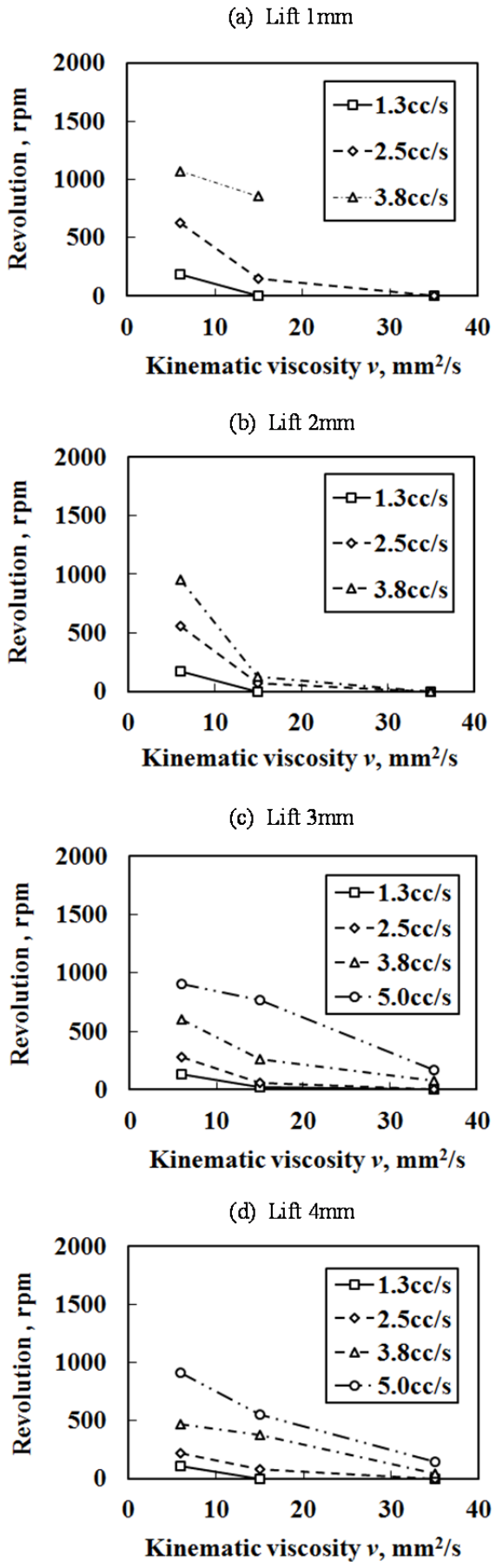

Fig. 7: *Relation between kinetic viscosity v and revolution*

This shows that the viscosity has a large effect when the lift is small and the fluid jet is at the top of the ball. In addition, when the lift is 3 mm or more, the rotational speed is greatly reduced at the low viscosity of 6 mm^2/s, and the check flow rate is small. At a viscosity of 15 or 35 mm^2/s, however, the rotational speed first increased and then later decreased as the lift increased. The reason the rotational speed changes greatly when the viscosity is high is thought to be due to there being times when the check ball is easily affectedby the swirling flow as the distance between the top of the ball and the inflow area changes depending on the initial position of the check ball. This showed there is a strong relationship between the check flow rate and the hydraulic fluid viscous force when the viscosity is high.

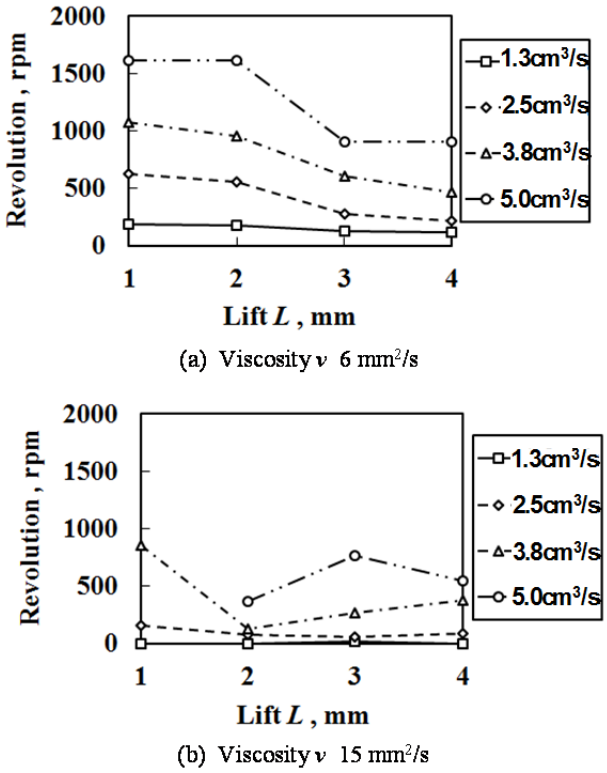

Fig. 8: *Relationship between revolution and lift L*

The test was conducted using Model 1, which has a ϕ 5 inflow in the center, and Model 2, which has a ϕ 2 inflow from the side that generates a swirling flow. The effect on the check flow rate and rotational speed of the kinetic viscosity at the respective positions was found, but the detailed state of the flow was unknown. Here, flow beads made by Sumitomo Seiko Chemicals that are low-density polyethylene particles with an average diameter of 11 μm and that have been alumite surface treated were added to the hydraulic fluid, and image processing using a high-speed camera was conducted to observe the flow around the check ball. The state of this flow is shown in Fig. 9. Fig. 9(a) shows the flow state for Model 1 at a lift of 2 mm, flow rate of 7.5 cm^3/s, and kinetic viscosity of 6 mm^2/s, and Fig. 9(b) show the flow state when the kinetic viscosity is changed to 35 mm^2/s. Also, Fig. 9(c) shows the flow state when the lift is 4 mm, the flow rate is 23.9 cm^3/s, and the kinetic viscosity is 6 mm^2/s, and Fig. 9(d) shows the flow state when the viscosity is changed to 35 m^2/s. These flow rates are the maximum values at

which the ball does not rise up. For Model 1, when the kinetic viscosity of Fig. 9(a) is a low 6 mm^2/s, a variety of flows, such as the back flow and swirling current at the top left of the ball or a flow going downward, were observed. However, when the kinetic viscosity is 35 mm^2/s as in Fig. 9(b), an upward flow that passes smoothly along the ball from the inlet to the outlet forms. In other words, it is thought that as the kinetic viscosity increases, the flow rate going downward decreases and the check flow rate increases. In addition, a flow going around the ball was observed at either viscosity, and this tendency was observed to be stronger at the low kinetic viscosity of 6 mm^2/s than at a high kinetic viscosity. Next, when the lift was 4 mm as for Fig. 9(c) and 9(d), it was observed that the fluid jet from the inlet was striking the top of the ball and that the reaction force that is changed by this main flow is thought to change to a downward direction on the ball. At this time as well, if the relative flow rate at a low viscosity is high, it was observed that a variety of flows formed around the ball and some of these flowed to the bottom of the ball and lifted it. At high viscosity, however, the flow was close to a uniform flow, which increased the check flow rate. From the above results it is thought that for the Model 1 center inflow that when the lift is small, the flow around the ball and the downward flow are relatively high and it is easy for an upward forced to be generated on the ball, so the difference from the viscosity is small, but as the lift becomes larger, the main flow strikes the top of the ball, which, especially at high viscosity, requires a large check flow rate.

Next, for Model 2, which actively generates a swirling flow, the flow state at a lift of 2 mm, a flow rate of 3.8 cm^3/s, and a kinetic viscosity of 6 mm^2/s is shown in Fig. 9(e), and that for a kinetic viscosity of 15 mm^2/s is shown in Fig. 9(f). Further, the flow state at a lift of 3 mm, flow rate of 3.8 cm^3/s, and kinetic viscosity of 6 mm^2/s is shown in Fig. 9(g), and that for a kinetic viscosity of 15 mm^2/s is shown in Fig. 9(h). Comparing Fig. 9(e) to Fig. 9(f) shows that a swirling flow is observed in both cases and that even at the same flow rate, the swirling flow decreases as the kinetic viscosity increases. There is also a large difference in the ball rotational speed, which Fig. 7(b) shows changes from approximately 1,000 rpm at a kinetic viscosity of 6 mm^2/s to approximately 90 rpm at a kinetic viscosity of 15 mm^2/s. When this lift is 2 mm, the flow directly strikes the center of the check ball, which blocks the flow and splits it upward and downward, and there is very little swirling flow. When the lift is 3 mm as shown in Fig. 9(g) and 9(h), the ball position is low, so the fluid jet from the inlet does not directly strike the ball and causes a large swirling flow. The ball rotational speed is approximately 700 rpm at a kinetic viscosity of 6 mm^2/s and approximately 250 rpm at a kinetic viscosity of 15 mm^2/s, so the difference is small.

Although a large difference was observed in the swirling flow, this is thought to be due to the viscous force of the hydraulic fluid not being very large and thus little of the force for rotating the ball is transmitted.

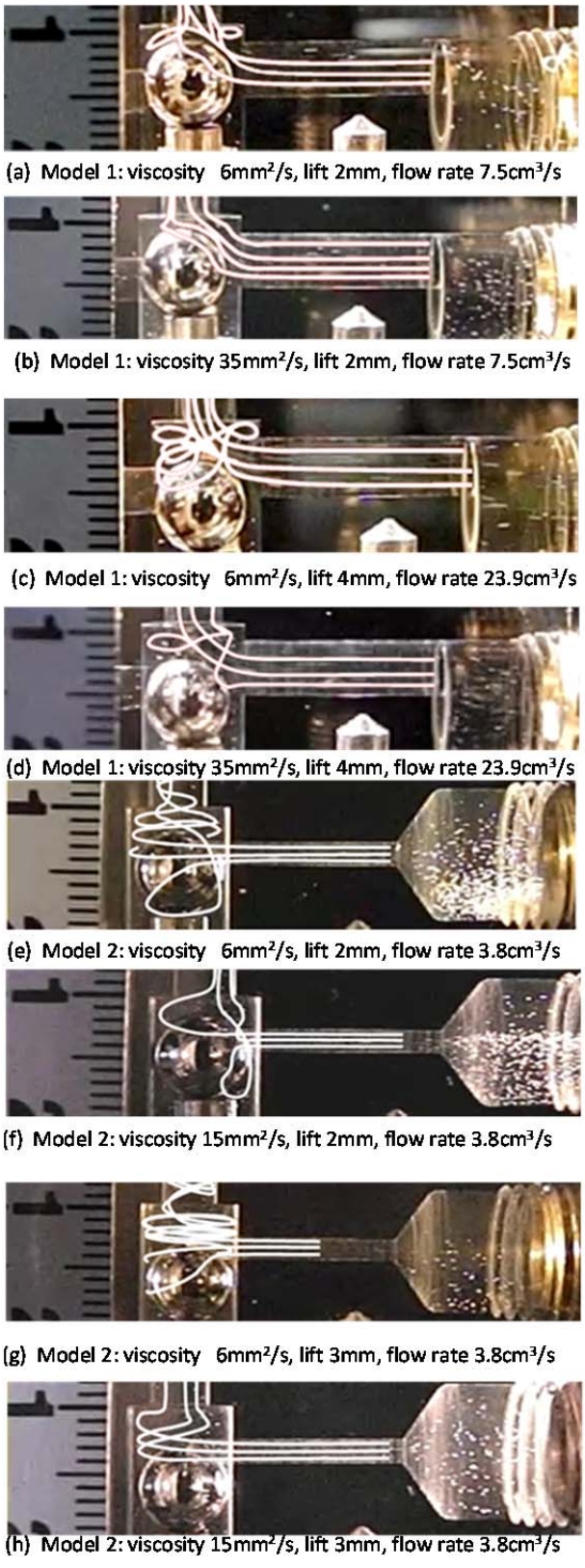

Fig. 9: *Flow pattern of Model 1 and Model 2*

The above results showed that when the lift is 2 mm or less, swirling flow is observed at low viscosities, but almost none is observed at high viscosities, so the high viscosity hydraulic fluid has a large effect on the ball upward force generated by the viscous behavior and thus the check flow rate decreases as the viscosity increases. Further, when the lift is 3 mm or higher a

swirling flow is generated regardless of the viscosity, but dissipation occurs in the vicinity of the ball, so it is assumed that the balance between the viscosity and the swirling flow is why no change in the check flow rate was observed.

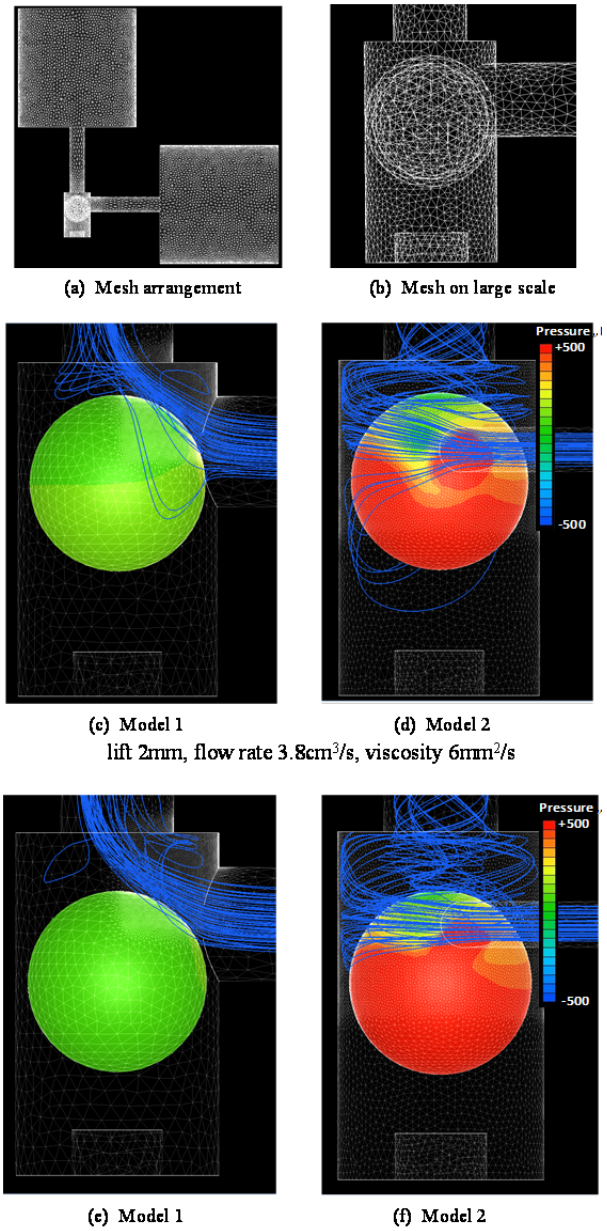

Fig. 10: *Mesh arrangement, Flow pattern and ball surface pressure*

4 Considerations

As a consideration, the thermofluid CAE analysis tool SCRYU/Tetra was used for analysis and the state of the flow was observed. Mesh arrengements were shown Fig. 10(a) and 10(b). Large tank inlet and outlet are provided to stabilize the flow of the tube-shaped L. Here the ends was set at its boundary condition A low Re k-ε model was used for the turbulent flow model and a no-slip condition was used for the wall surface condition. Eight layers of 1.5×10^{-4}m thick boundary layer mesh were inserted to improve the resolution of the separation and reattachment in the vicinity of the wall surface, etc. Mass flow rate specification was used for the inflow condition and natural inflow and outflow conditions were used for the outflow condition. For the mesh preparation, the area from the inflow opening to the ball vicinity was observed very carefully and a steady analysis was conducted using an approximately 3 million mesh partition number. The resulting flow pattern and ball surface pressure distribution are shown in Fig. 10(c) to 10(d). However, Fig. 10(c) is for Model 1 using a lift of 2 mm, flow volume of 3.8 cm^3/s, and kinetic viscosity of 6 mm^2/s, and Fig. 10(d) is for Model 2 using the same conditions. Further, Fig. 10(b) is for Model 1 using a lift of 4 mm, flow volume of 3.8 cm^3/s, and kinetic viscosity of 6 mm^2/s, and Fig. 10(f) is for Model 2 using the same conditions. First, for Model 1 with a lift of 2 mm as shown in Fig. 10(c), the concentration of streamlines on the top of the ball creates a high surface pressure on the area struck by the fluid jet and acts as a downward reactive force on the ball. Further, it was found that the surface pressure on the side of the ball at this time was small. For Model 2 in Fig. 10(b), the ball surface pressure was high at the bottom and low at the top, so it is presumed the net hydrodynamic force is generating an upward force. When the lift was 4 mm as for Fig. 10(c) and 10(d), this was more marked, and for Model 1 in Fig. 10(c) a downward flow from the streamline was observed. For Model 2 in Fig. 10(d), however, the positive portion of the ball surface pressure increased more than when the lift was 2 mm and so it is expected that the ball lifting force will increase. These results show that in Model 1 as the lift becomes larger, it becomes more difficult for the fluid jet to raise the ball, but in Model 2 the effect is very small because the fluid jet directly strikes the ball. The flow pattern of the experiment and CFD matched each other. It can be seen that the ball is moved by the surface pressure of the ball. In the future, We think we want to help in the design to verify the accuracy of the CFD.

5 Conclusions

The objective of this research is to realize hydraulic ball valves that do not use a spring, and tests were conducted to measure the check flow volume and rotational speed under different hydraulic fluid inflow positions, inlet diameters, ball positions, and hydraulic fluid kinetic viscosities as well as to visualize the flows in the vicinity of the ball. The results showed that using inflow from the side to actively cause a swirling flow made it possible to raise the ball at low flow volumes. Further, a high-speed camera was used to observe the particles in the fluid to consider reasons for improvement. However, since the various parameters, such as swirling flow strength, relative position to the ball, inlet diameter that determines the fluid jet strength, hydraulic fluid viscosity, etc., mutual act on each other, in the future we plan to use CAE analysis to deepen our understanding of the phenomena and conduct quantitative observations.

Our main conclusions are summarized as follows.

- Changing the flow volume, kinetic viscosity, and lift while studying the check flow volume showed there is a mutual relationship among the check flow volume, ball initial position, and kinetic viscosity.
- Using a shape where the inflow is from the side generates a swirling flow and greatly reduces the check flow volume compared to center inflow; making possible a check flow volume below 8.3 cm^3/s.
- The model with center inflow demonstrated a check flow volume of about 20 cm^3/s at a lift of 3 mm or less, but at a lift of 4 mm the phenomenon changed so that sometimes a check flow volume of 50 cm^3/s is required.
- In the model with center inflow, at a lift of 1 mm or 3 mm, if the kinetic viscosity is high, the ball rises easily and the check flow volume is small. At a lift of 4 mm, this balances with the force on the ball from the fluid jet to determine the check flow volume.
- When the inflow is from the side and the kinetic viscosity is changed, the ball rotational speed and the strength of the swirling flow become larger, but there is almost no change in the check flow volume.

Nomenclature

Q	Volumetric flow rate	[cm^3/sec]
L	Lift	[mm]
ν	Kinetic viscosity	[mm^2/s]

References

Grossschmidt, G. and **Harf, M.** 2009. COCO-SIM Object-Oriented Multi-Pole Modelling and Simulation Environment for Fluid Power Systems, Part 1: Fundamentals. *International Journal of Fluid Power, August Issue.*

Hayase, T., **Humpherey, J.A.C.** and **Greif, R.** 1992. A Consistently Formulated QUICK Scheme for Fast and Stable Convergence Using Finite-Volume Iterative Calculation Procedures. *J. Comput. Phys*., Vol. 98 - 1, pp. 108 - 118.

Hong, F. G. Xin, **Huayong, Y.** and **Tsukiji, T.** 2002. Numerical and experimental investigation of cavitating flow in oil hydraulic ball valve. *Proc. of 5th JFPS International Symposium on Fluid Power, NARA*2002, Vol. 3, pp. 923 - 928.

Tsukiji, T. and **Suzuki, Y.** 1996. Numerical Simulation of an Unsteady Axisymmetric Flow in a Poppet Valve Using the Vortex Method. *ESAIM*(*European Series in Applied and Industrial Mathematics*), Vol. 1, pp. 415 - 427.

Shinji Kajiwara
Brief Biographical History:
1993- Hitachi Zosen Co., Ltd
2001- Daihatsu Motor Co., Ltd
2005- Kinki University
Membership in Academic Societies:
• The Japan Society of Mechanical Engineers (JSME)
• The Japan Fluid Power System Society(JFPS)
• The Society of Automotive Engineers of Japan(JSAE)